ARMA 16-191

Reducing breakdown pressure and fracture tortuosity by in-plane perforations and cyclic pressure ramping

Simon Falser, Weijian Mo
Shell Projects & Technology, Beijing, China
Dingwei Weng, Haifeng Fu, Yongjun Lu, Yunhong Ding
RIPED-Langfang of PetroChina, Langfang, China
Sau-Wai Wong
Shell International Exploration & Production, Houston, USA

ABSTRACT: Formation breakdown failures were early on identified as technical risk in hydraulic fracturing treatments of wells in the Sichuan basin, China. This study focuses on reducing the breakdown pressure while improving near-wellbore fracture geometries by a variety of perforation geometries as well as cyclic pressure ramp-ups. A total of six large scale polyaxial experiments on isotropic cement samples were conducted, in which the principal stresses were set to represent a horizontal wellbore in a normally faulted stress regime. The results show that breakdown pressures can be reduced by 25% with in-plane perforations or cyclic pressure ramping. The results further indicate that open hole and conventional plug-and-perf completions lead to more near wellbore fracture tortuosities, while transverse fractures can be initiated from the in-plane perforation geometry.

1. INTRODUCTION

Most operators active in unconventional resource plays base their hydraulic fracturing treatment design on their experiences gained in North America's normally faulted marine basins. In areas with more challenging tectonic settings and deeper targets, however, hydraulic fracturing treatments need to be designed for higher breakdown pressures, higher average pumping pressures, and the risks of limited fracture height growth as well as pre-mature screen-outs.

In China's Sichuan Basin, breakdown pressures exceeding the design pressure rating of available standard pumping equipment (15 kpi surface pressure limit) have caused the failure of numerous hydraulic fracturing stages, or required additional perforations or sand jetting before the formation would break down.

In addition to issues related to breakdown pressure, non-radioactive tracer logs and micro-seismic data indicated very limited fracture heights. It might be possible that at certain formation layers, the hydraulic fractures were propagating horizontally. This hypothesis is reinforced by the closure stresses of several injection tests, which yielded a theoretical minimum horizontal stress equivalent to the overburden stress [1]. This suggests a strike-slip ($\sigma_H > \sigma_v > \sigma_h$) to reversely faulted stress regime ($\sigma_H > \sigma_h > \sigma_v$). When stimulating horizontal wells drilled on σ_h azimuth in such settings, the hydraulic fractures initiate along the sides of the wellbore where the hoop-stress σ_θ governed by $\sigma_H >> \sigma_v$ is minimum. As the fracture then propagates into the principal stress governing zone away from the wellbore, two factors inhibit its re-orientate into the vertical plane: first, the marginal stress anisotropy σ_v - σ_h accommodates either orientation and therefore does not act as the required restoring force, and second, the laminated fabric of these shale formations favours horizontal fractures parallel to its bedding plane.

Even in normally faulted stress regimes, hydraulic fractures typically initiate non-transversely from horizontal wells, before re-orientating itself perpendicularly to the minimum principal stress further away from the wellbore (Fig. 1, left). These fracture tortuosities are undesirable, as they increase the average treating pressure and the risk of pre-mature screen-outs during pumping of the designed pad, and they also potentially impact the wellbore-to-fracture connectivity during production. It would therefore be highly desirable to initiate transverse fractures right at the horizontal wellbore, and extend them into the far field as shown schematically in Fig. 1 (right).

Transverse fracture initiations, in combination with breakdown pressure reduction measures, are both the focus of this paper.

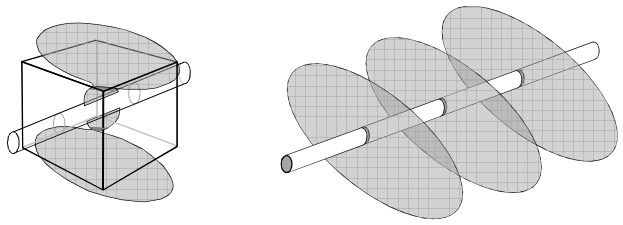

Fig. 1: Undesirable fracture tortuosities: caused by the transition between near-wellbore and far field stress regime (left); transverse fractures reaching from the wellbore into the far field (right).

1.1. Theoretical breakdown pressure models

The theoretical breakdown pressure models $P_{b,th}$ in the literature vary widely, depending on the assumptions they are based upon. The following models are stated for horizontal wells drilled in the minimum principal stress direction (σ_h-azimuth) and in a normally faulted stress regime. For other wellbore azimuths or stress regimes, their principal stresses need to be updated accordingly. A complete solution to the general equations is given by Huang et al. [2]. The most widely used simplification is by Willis and Hubbert [3] and given in equation (1). It differentiates between fast- and slow pressurisation rate, with the difference being that in fast pressurisation, fluid is injected at a rate at which the pore pressure is not able to equilibrate with the fluid pressure in the wellbore, while in the slow pressurisation it is.

$$P_{b,th,fast} = 2P_{b,th,slow} = 3\sigma_H - \sigma_v + T \qquad (1)$$

Where σ_H and σ_v are the intermediate- and maximum pronciple stresses, and T is the rock's tensile stregth.
The Haimson and Fairhurst [4] model given in equation (2) extended the fast pressurisation case of equation (1) by accounting for the Biot effect:

$$P_{b,th,Biot} = \frac{3\sigma_H - \sigma_v + T - 2\eta p_0}{2(1-\eta)}; \qquad \eta = \frac{\alpha(1-2\nu)}{2(1-\nu)} \qquad (2)$$

Where p_0 is the pore pressure, ν the Poisson's ratio and α the Biot coefficient. The model by Hoek and Brown [5] in equation (3) is similar to the slow pressurisation version of equation (1), with the term ($5/6*\sigma_H + T$) replaced by the compressive strength term $\sigma_c/2$, where σ_c is the unconfined compressive strength:

$$P_{b,th,\tau} = \frac{2}{3}\sigma_H - \frac{1}{2}\sigma_v + \frac{1}{2}\sigma_c \qquad (3)$$

The models (1) to (3) assume a cylindrical wellbore without notches or imperfections, and are therefore no longer strictly applicable to perforated wellbores. A model which does account for a starter fracture [6] is given in equation (4):

$$P_{b,th,FM} = \frac{K_{IC} - g(a/R_w)\sqrt{\pi a}(\sigma_v - \sigma_H)}{\sqrt{\pi a}\ f(a/R_w)} \qquad (4)$$

Where R_w and a are the wellbore radius and the initial crack length respectively, K_{IC} is the mode I fracture toughness, while the values for $g(a/R_w)$ and $f(a/R_w)$ are tabulated with respect to the relative orientation to the principal stress directions. The model suggests that the breakdown pressure decays exponentially with increasing starter crack length, which shall be one of the investigation points in this study.

1.2. Fracture reorientations

There are few studies devoted to the reorientation of a fracture while propagating from the wellbore into the far field. Lecampion et al. [7] describe it based on a the critical disturbance length γ^*, after which less energy is required to propagate a transverse rather than an axial fracture (see Fig. 2).

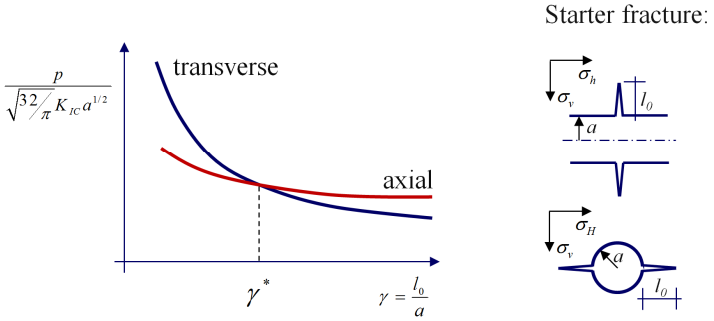

Fig. 2: theoretical fracture reorientation criterion (left) with the hypothetical starter notch configurations (right) [7].

When their model was applied to three field cases, it predicted the fracture to turn into a transverse orientation within one wellbore radius.
Other theoretical models describe the transition between the wellbore and the far field as gradual fracture curving [8], but experimental results have shown that the transition usually occurs in a less gradual and more abrupt way [9].

2. IN-PLANE PERFORATION CONCEPT

The fundamental questions to be addressed in this study are whether reductions in breakdown pressure and fracture tortuosities can be achieved by:

- an in-plane perforation strategy
- A cyclic pressure ramp-up

The aim is first to investigate whether the pressure required for formation breakdown is dependent on the length of the perforation tunnels. The basic idea is to bypass near wellbore stress concentrations by perforating deeper into the formation, as suggested

theoretically and on the basis of a starter fracture in equation (4), but which has yet to be confirmed by experimental data.

The second point of investigation is the fracture initiation: if deep perforations phased 60° in a single plane are considered holes which fail once their hoop stress exceeds the rocks tensile strength (mode I fracturing), they could potentially link up radially and create a transverse fracture right from the wellbore. This is shown schematically in Fig. 3. If this scheme is successful, it would be beneficial on two fronts:

- Reduce breakdown pressure
- Improve near-wellbore fracture geometry

A better connectivity reduces the average treating pressure during a hydraulic fracturing job, which directly lowers the pumps' fuel cost and reduces their wear-and-tear. A better fracture to wellbore connection would also facilitate the ease of proppant placement and enhance the overall well productivity. Reducing the breakdown pressure, on the other hand, enables the optimisation of the required pumping capacity to be installed for the treatment execution, which again has significant potential for cost savings. In basins with excessive tectonic stresses, such a perforation scheme can become an enabler to stimulate well stages which otherwise would have to be left untreated. The experimental verification of this concept is presented in section 3.

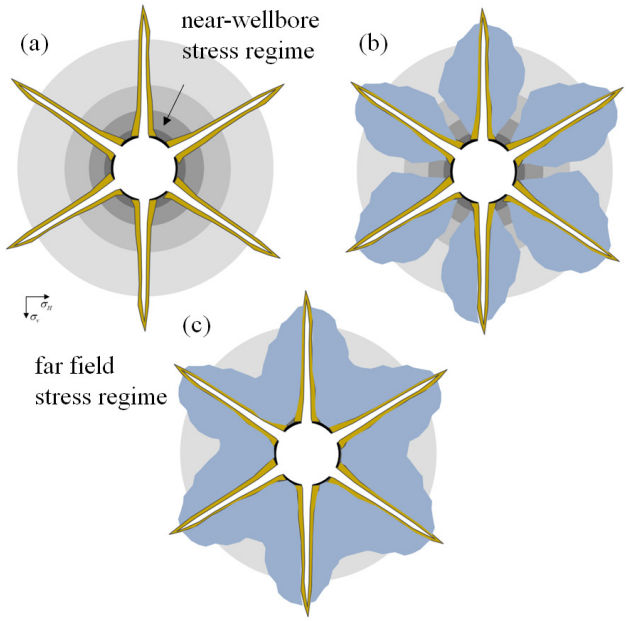

Fig. 3: schematics of: in-plane perforations penetrating into the far field stress regime (a); hoop-stress failure of perforation tunnels initiating fractures in a single plane (b); circumferential linking up of fractures, merging into a single transverse fracture (c).

3. EXPERIMENTAL VERIFICATION

To verify this in-plane perforation concept, an experimental testing program in a large-scale polyaxial apparatus was undertaken.

Unlike field trials, in polyaxial experiments, the material properties, completion geometry, principal stress conditions as well as the fluid properties and injection rate can be accurately designed and controlled. Apart from pressure recordings, the fracture geometry can be investigated by post-test cuts of the sample, on which surfaces the dyed injection fluid can be traced back. The sequence of the fracture propagation can in turn be monitored in real time based on acoustic emission recordings.

The sample dimensions and major specifications of the polyaxial laboratory and test set-up are given in Table 1, while further details about the apparatus can be found in [10]. It is one of very few polyaxial testing facilities designed for samples of that scale, and it is therefore ideally suited to investigate near wellbore fracture geometries unaffected by the outer fixed boundary constraint.

Table 1: Sample size and apparatus specification.

Specimen size [mm]	762 x 762 x 914
Max. injection rate [ml/min]	15000
Min injection rate [ml/min]	5
Max. injection pressure [MPa]	82
Max. stress [MPa]	69
Acoustic emission channels	24

The samples were formed of a cement mixture to ensure fabric consistency and thus comparability of all experiments. Standard grade wellbore cement was used, with additives for strength and to inhibit air inclusions. The wellbores were formed by casting standard 2-7/8 inch tubings into the samples' centre. Styropor dummies of specific geometries were connected to pre-drilled holes in the casing, and once the sample was set, these dummies were dissolved by acid, forming the perforation tunnels. It is recognised that in-situ gun-perforating would result in additional stress caging and damaged surface around the perforation tunnels. The absence of these effects in the polyaxial experiment is a limitation, as gun-perforating the samples under stress conditions was not deemed practical for safety reasons, and perforating under no-stress conditions would lead to a different local stress state and sample damage.

Because the total sample preparation time, from the initial casting to the installation of acoustic sensors and the final rigging up, was on average 8 weeks, the data quality from each experiment was of paramount

importance, given the substantial equipment and labour costs involved.

Scaling hydraulic fracturing experiments is non-trivial, as it encompasses geometry, mechanical properties of the fabric, fluid properties and injection rate. According to De Pater [11], the fracture toughness scale is proportional to the length scale squared, which in this study is avoided by keeping the wellbore in true scale. It is further suggested to inject high viscosity fluid at a low rate, since their products are proportional to the third power of the length scale.

The mechanical sample properties were as follows: Young's modulus E = 12.5 GPa, Poisson's ratio ν = 0.19 and density ρ = 1.87 g/cm^3. Linear gel with a dynamic viscosity of 105 cP was injected at 60 ml/min.

The wellbore was mimicking a horizontal well in a normally faulted stress regime and the applied principle stresses given in Table 2 were kept constant for all tests.

Table 2: Principal stresses applied in all tests.

[MPa]	σ_v	σ_H	σ_h
	30	27	19

3.1. Polyaxial testing series

The first investigation point was to compare the breakdown pressures and near wellbore fracture geometries of an open hole completion, a plug-and-perf completion and the novel long and in-plane perforation scheme. The open hole experiment (T1) serves as the base case and represents a field completion with uncemented sliding sleeves. The plug-and-perf completion (T2) is designed in a way that its perforations are short enough to only reach into the near wellbore region in which the stresses along the $\sigma_{\theta,\ max}$ axis are higher than in the far field. The long in-plane perforation experiment (T3) is the novel design highlighted in Fig. 3, which is expected to demonstrate the theoretical improvements with regards to fracture geometry and breakdown pressure.

After conducting the first set of experiments, the second point of investigation was to see whether potential breakdown pressure reductions are caused by the perforation length or its in-plane geometry. An experiment with a short and in-plane perforation geometry was therefore conducted (T4).

To see whether the breakdown pressure can be reduced despite a conventional perforation completion, an experiment was conducted in which the pressure was ramped up cyclically until fracturing was initiated (T5). The details of these experiments are given in Table 3.

Table 3: Polyaxial tests of this study with their respective completion design and normalised penetration depth.

No.	*Test description*	L/D_w
T1	open hole	0
T2	short 6spf 60° phased	0.5
T3	long in-plane	3
T4	short in-plane	0.5
T5	cyclic P ramping, 6 spf	0.5

4. POLYAXIAL TEST RESULT

This experimental result section focuses on two major aspects: the break-down pressure (P_b) signatures shown in Fig. 4, and the near wellbore fracture geometries given in Fig. 5. The breakdown pressure histories given in Fig. 4 (B) are normalised by the minimum principal stress (σ_h =19 MPa), to make their differences more pronounced and their comparability easier.

In test T1, the open hole experiment, a sharp decrease in fluid pressure was noted once the breakdown pressure $P_{b,T1}$ was reached. Comparing that with the resulting fracture geometry of T1 given in Fig. 5 (B), it can be seen that the fracture initiated along the wellbore axis, but then the fracture plane reoriented itself sharply to be perpendicular to the direction of σ_h, highlighted as secondary transverse fracture. Its breakdown pressure $P_{b,T1}$ exceeded the minimum principal stress by 4.3 MPa.

The breakdown pressure of the short in-plane (T2) perforation geometry was with $P_{b,T2}$ = 6 MPa about 1.7 MPa higher than that in the open hole test. The experiment's pressure signature after breakdown is comparatively less sharp, indicating a difference in the fracture initiation process. Looking at its near-wellbore fracture geometry, it can be seen that only 3 of the 6 perforations took fluid and initiated fractures. Numbering them from the bottom (#1) to the top (#6), it was noted that #2 propagated a transverse fracture, while #6 initiated a transverse fracture but was arrested locally. Fig. 5 (A) shows that perforation #4 initiated an axial fracture with complex branching around it. Two observations indicate stress interference between the axially spaced perforation tunnels: first, fractures were initiated only from alternate perforations (#2, #4 and #6), and second, a complex fracture was initiate from perforation #4, which is located in between the transverse fractures and therefore exposed to a stress shadow from both sides. These observations are further consistent with a currently ongoing testing programme.

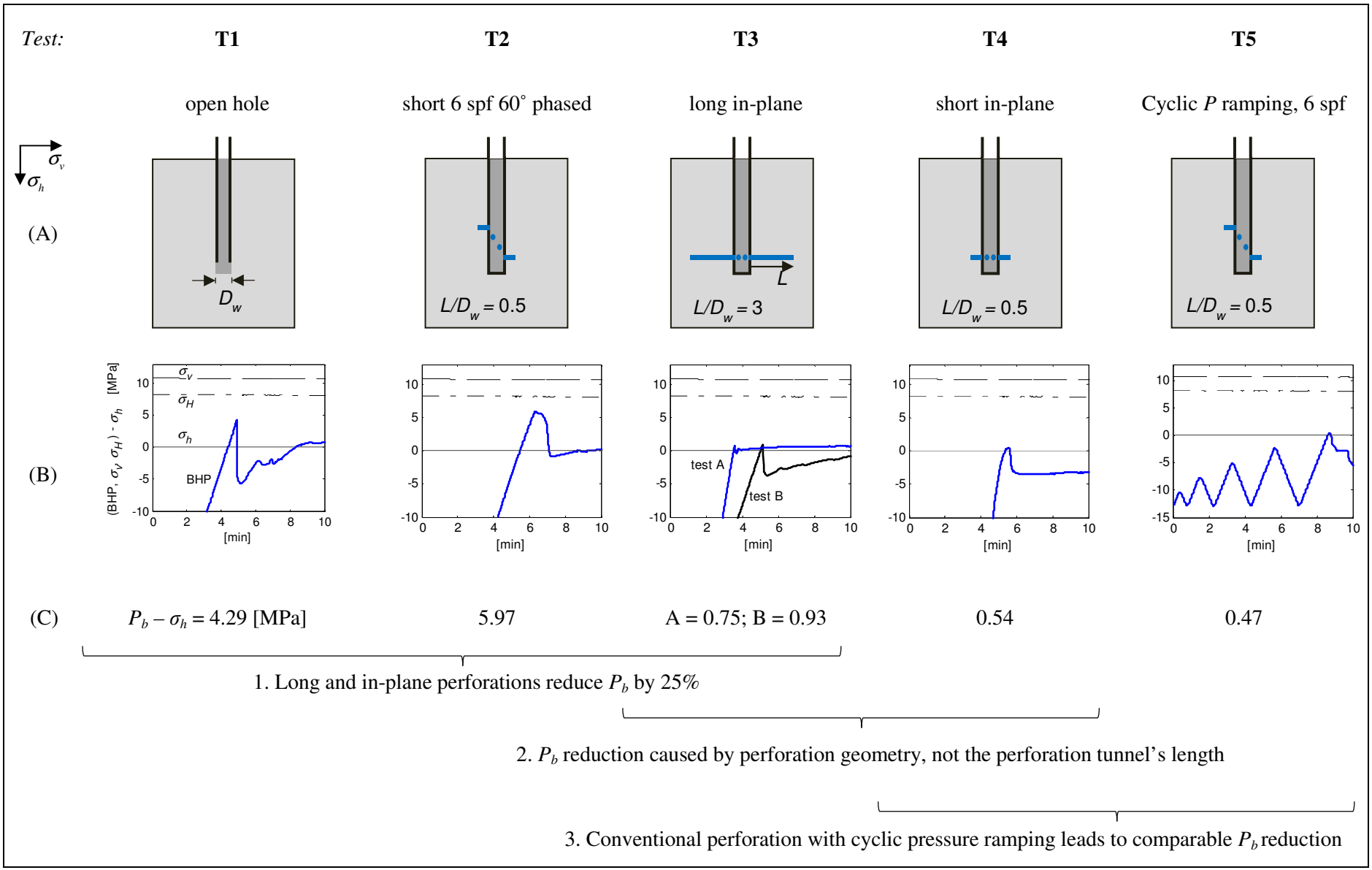

Fig. 4: Completion geometries (A) and their respective pressure curves (B) with normalised breakdown pressure P_b (C).

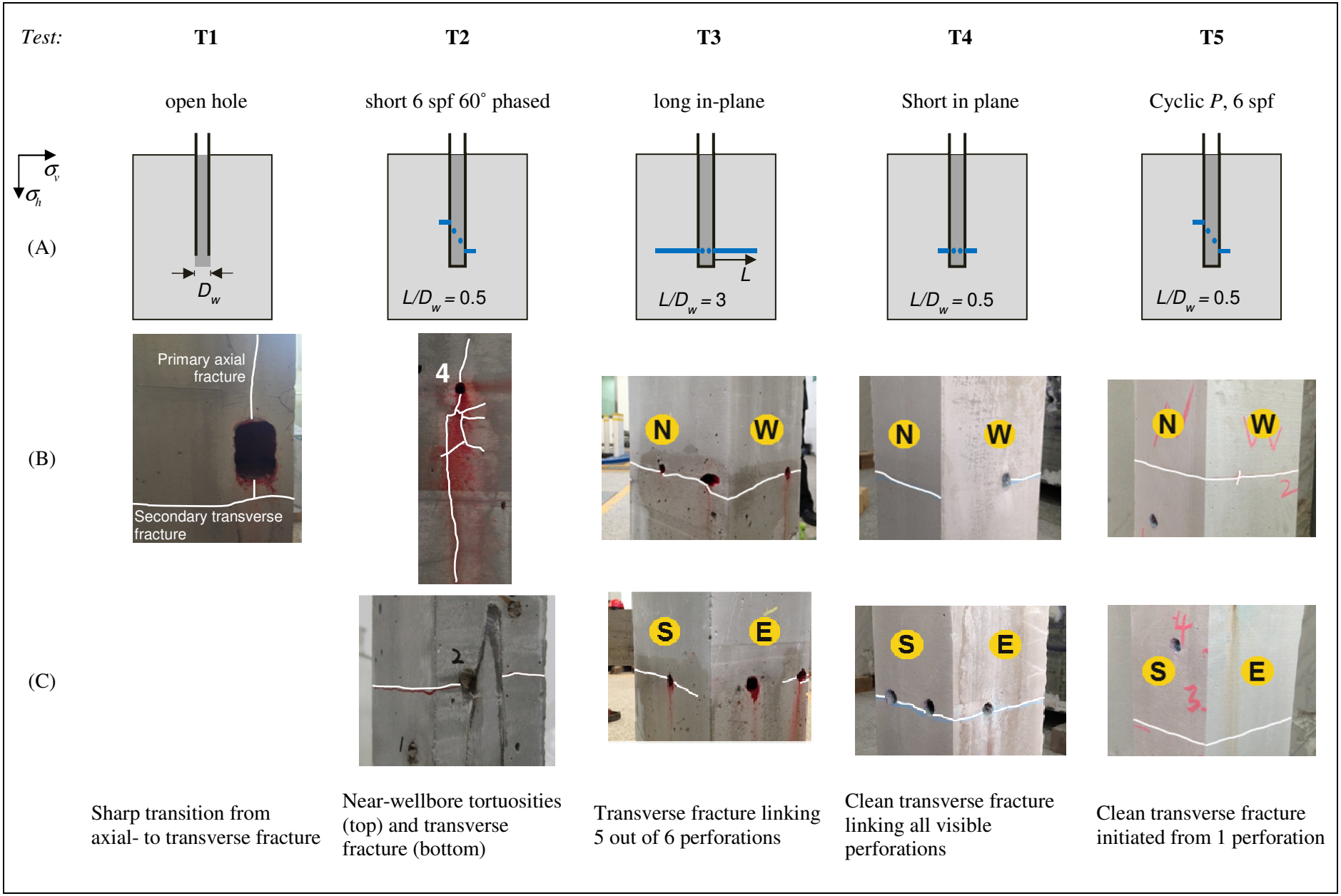

Fig. 5: Completion geometries (A) and their respective near-wellbore fracture geometries (B-C).

Because the experiment with long in-plane (T3) completion geometry was to demonstrate the design's benefits, two identical tests with the same geometry were carried out to show repeatability and consistency of the results. Both experiments show a distinct reduction in breakdown pressure (Fig. 4, C), which in both cases exceeds σ_h by only less than 1 MPa. These results already show that P_b can be reduced by about 25% with an in-plane and long perforation geometry. Referring to the fracture geometry of T3, it can be noted that all 6 perforation tunnels took fluid, of which 5 initiated a transverse fracture. Fig. 5 (B-C) shows that they linked up circumferentially except for the perforation in South-East direction from which no fracture was initiated. The acoustic events given in Fig. 6 further indicate that the fractures have initiated in a single plane but individually from each perforation. It can be further noted that the locations of the acoustic events are in line with the visually observed circumferential fracture highlighted in red.

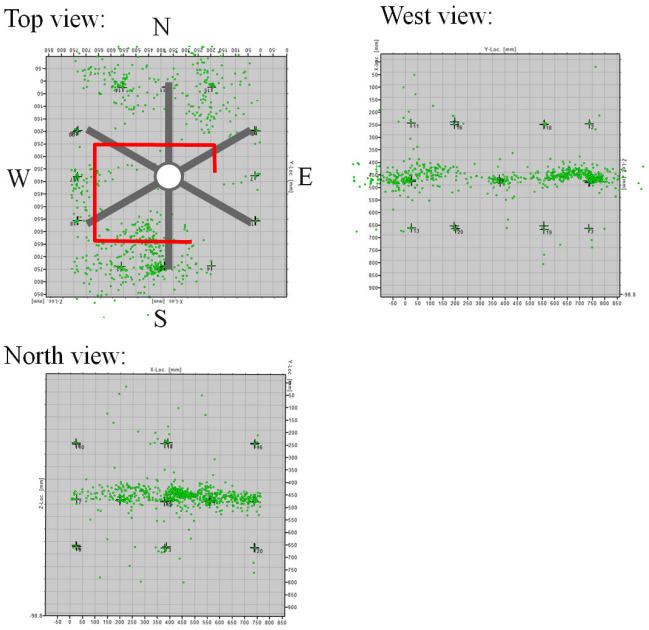

Fig. 6: Acoustic events with respect to the perforation tunnel orientation (grey) and the continuous circumferential fracture (red).

To determine whether the reductions in breakdown pressure were caused by the in-plane geometry or by the perforation tunnels' length, an experiment with a short in-plane (T4) fracture geometry was conducted. The results show that its breakdown pressure ($P_{b,T4}$ = 0.54) was comparable with both experiments in T3, which led to the conclusion that the P_b reductions are caused by the in-plane geometry rather than the perforation length. Furthermore, the resulting fracture initiated transversely and linked up – similar to T3 – over most of the wellbore's circumference (see Fig. 5 (B-C)).

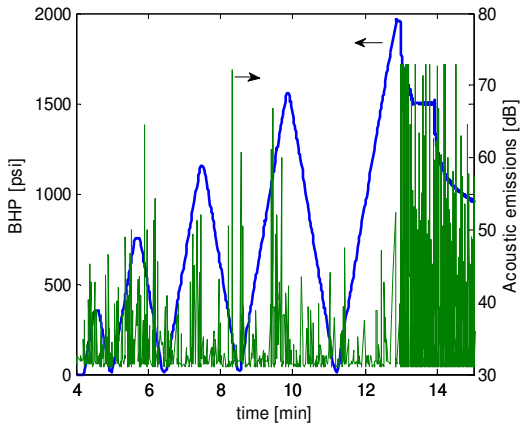

Fig. 7: Acoustic emissions (green) during the cyclic pressure ramping (blue)

The last investigation point in this study was to see whether the breakdown pressure in a conventional perforation geometry (6 spf, same as in T2) can be reduced by cyclic pressure ramping. It is standard practice in field application where breakdown issues are encountered to cycle the pumping pressure monotonously around the installed design capacity. In this experiment (T5), however, the pressure was increased with each load cycle, while the pressurisation rate *dP/dt* was kept constant. The acoustic signals recorded (see Fig. 7) with each pressure cycle indicate that pressure ramping weakens the near-wellbore formation. The cause of this may be due to excess pore pressure dissipation, but a more detailed analysis of the phenomena will be published subsequently. As a result, the breakdown pressure is reduced to levels observed in the preceding in-plane geometry tests (T3 and T4). From the fracture geometry in T5, it is observed that only one perforation tunnel took fluid, initiated a short vertical fracture (see Fig. 5 (B) West), but propagated a single transverse fractures. That may imply that the cyclic stimulation has the greatest impact on the weakest fluid-rock contact point, from which it eventually initiates a fracture, avoiding multiple initiations and therefore stresses interactions between perforations.

4.1. Experimental vs. theoretical P_b

The recorded breakdown pressures in the experiments can now be compared to the theoretical P_b models presented in section 1.1. The two plots in Fig. 8 show the same data, with the lower graph being a zoomed-in view of the upper graph. In the upper graph it can be seen that due to the exponential decay of the minimum hoop stress σ_θ, its magnitude at the depth of the short perforation is significantly larger than at the depth of the long perforation, again showing that the tests with short perforations (T2, T4 and T5) are confined to the hoop-stress dominated near wellbore region.

Fig. 8 (bottom) shows that the breakdown pressures of the open hole experiment ($P_{b,T1}$) and short 6 spf test (*P*-

$_{b,T2}$) are in agreement with the slow pressurisation model given in equation (1) and shown as $P_{b,th,slow}$. The assumption of slow pressurisation rate is acceptable, since the product of rate and fluid viscosity is about 10^3 lower in the experiments than that of an average field case. The model based on fracture mechanics (equation (4)) was applied with a toughness of K_{IC}=0.5 MPa(m)$^{1/2}$, on azimuth with σ_h (θ = 0), and for both a long and a short starter crack a/R_w = 0.5…3, but for the conditions the model turned out to be insensitive to the initial fracture length, and is again in agreement with the breakdown pressures of T1 and T2.

The experiments in which the breakdown pressure was successfully reduced to within 1 MPa of σ_h, are best represented by the model given in equation (3) and assuming an average compressive strength of σ_c = 50 MPa, but more tests with samples made of materials with a variety of compressive strengths would be required to claim the model's applicability for breakdown pressure estimates in such geometries.

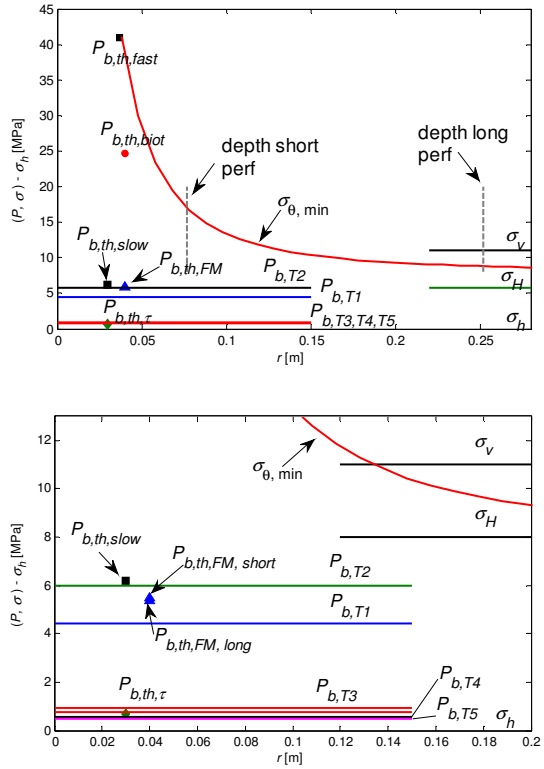

Fig. 8: Actual breakdown pressures of T1 – T5 in comparison with the theoretical models in equations (1) – (4); σ_h-normalised principal stresses σ_v, σ_H, and the minimum hoop stress σ_θ. The bottom figure is a zoomed-in view of the top figure.

4.2. Numerical validation

A newly developed hydraulic fracturing simulator was applied to simulate the polyaxial experiment with the open-hole configuration (T1). The fully 3D boundary element code [12] was able to capture the scale and boundary conditions adequately. A more detailed description of the modelling workflow can be found in [13]. Comparing the pressure evolutions in Fig. 9 of both the experiment (black) and the simulation (orange), it can be seen that the unstable fracture propagation post breakdown cannot be captured numerically, but once energy equilibrium is reached, the stable fracture propagation can be replicated in line with the changes in injection rate (dashed lines).

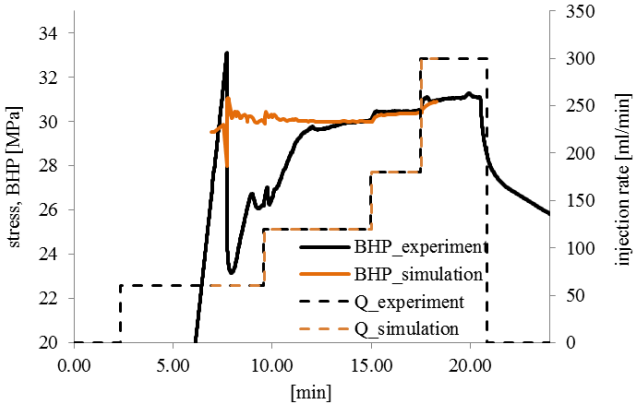

Fig. 9: Numerical simulation of the open hole experiment (T1).

CONCLUSIONS

The test series shows that breakdown pressures and fracture tortuosities can be reduced with an in-plane perforation strategy, and the application of cyclic pressure ramping. Three experiments with in-plane perforations led consistently to a 25% lower P_b as compared to the open-hole and conventionally perforated base experiments. Since the creation of in-plane perforation geometries downhole is impractical with readily available guns, further experiments are required to confirm that the same concept is applicable to cemented single entry completions. The cyclic pressure ramping technique through conventional perforations, however, could be readily deployed in the field, and thus shows great potential. Analysis of cyclic pressure ramping on wellbore rock's tensile breakdown will be the subject of a future publication.

ACKNOWLEDGEMENT

The insights from numerous technical discussions held with Alexei Savitski, Mikhail Geilikman, Gene Scott, John Dudley, Alexander Nezich, as well as with Tiancheng Liang and Nailing Xiu from CNPC greatly contributed to this study. The managerial support from Claudia Hackbarth, Yuzhang Liu and Caineng Zou is kindly acknowledged.

REFERENCES

[1] R. Yuan, L. Jin, C. Zhu, M. Zhou, and S. Vitthal, "Vertical or Horizontal?-Hydraulic Fracture Geometry as a Make or Break to a Tight Gas Field in the Western Sichuan Basin," in *IPTC 2013: International Petroleum Technology Conference*, 2013.

[2] J. Huang, D. Griffiths, and S.-W. Wong, "Initiation pressure, location and orientation of hydraulic fracture," *International Journal of Rock Mechanics and Mining Sciences,* vol. 49, pp. 59-67, 2012.

[3] D. Willis and D. Hubbert, "Mechanics of hydraulic fracturing," *AIME Trans,* vol. 210, pp. 153-168, 1957.

[4] B. Haimson and C. Fairhurst, "Initiation and extension of hydraulic fractures in rocks," *Society of Petroleum Engineers Journal,* vol. 7, pp. 310-318, 1967.

[5] E. Hoek and E. Brown, "Practical estimates of rock mass strength," *International Journal of Rock Mechanics and Mining Sciences,* vol. 34, pp. 1165-1186, 1997.

[6] X. Jin, S. Shah, B. Hou, and J.-C. Roegiers, "Breakdown Pressure Determination - A Fracture Mechanics Approach," *SPE Annual Technical Conference and Exhibition,* 2013.

[7] B. Lecampion, S. Abbas, and R. Prioul, "Competition Between Transverse And Axial Hydraulic Fractures In Horizontal Wells," *SPE Hydraulic Fracturing Technology Conference,* 2013.

[8] X. Zhang, R. Jeffrey, A. Bunger, and M. Thiercelin, "Initiation and growth of a hydraulic fracture from a borehole under toughness-or viscosity-dominated conditions," in *44th US Rock Mechanics Symposium and 5th US-Canada Rock Mechanics Symposium*, 2010.

[9] L. Weijers and C. d. Pater, "Fracture reorientation in model tests," in *SPE Formation Damage Control Symposium*, 1992.

[10] Y. Liu, M. Cui, Y. Ding, Y. Peng, H. Fu, Y. Lu*, et al.*, "Experimental Investigation of Hydraulic Fracture Propagation in Acoustic Monitoring Inside a Large-Scale Polyaxial Test," in *IPTC: International Petroleum Technology Conference*, 2013.

[11] C. De Pater, M. Cleary, T. Quinn, D. Barr, D. Johnson, and L. Weijers, "Experimental verification of dimensional analysis for hydraulic fracturing," *Old Production & Facilities,* vol. 9, pp. 230-238, 1994.

[12] G. Xu and S.-W. Wong, "Interaction of multiple non-planar hydraulic fractures in horizontal wells," in *IPTC 2013: International Petroleum Technology Conference*, 2013.

[13] S. Falser, A. Nezich, L. Nas, and Y. Yang, "Application of a new hydraulic fracturing simulator in Changbei II, Ordos Basin, P.R. China," *SPE 176927,* 2015.